

# Seismic performances of three- and four-sided box culverts: A comparative study

Qiangqiang Sun<sup>\*1</sup>, Da Peng<sup>2</sup> and Daniel Dias<sup>1,3</sup>

<sup>1</sup>Laboratory 3SR, Grenoble Alpes University, Grenoble, France

<sup>2</sup>Department of Civil and Environmental Engineering, University of Cincinnati, Cincinnati, U.S.A.

<sup>3</sup>School of Automotive and Transportation Engineering, Hefei University of Technology, Hefei, China

(Received March 25, 2020, Revised May 20, 2020, Accepted May 23, 2020)

**Abstract.** Studying the critical response characteristics of box culverts with diverse geometrical configurations under seismic excitations is a necessary step to develop a reasonable design method. In this work, a numerical parametric study is conducted on various soil-culvert systems, aiming to highlight the critical difference in the seismic performances between three- and four-sided culverts. Two-dimensional numerical models consider a variety of burial depths, flexibility ratios and foundation widths, assuming a visco-elastic soil condition, which permits to compare with the analytical solutions and previous studies. The results show that flexible three-sided culverts at a shallow depth considerably amplify the spectral acceleration and Arias intensity. Larger racking deformation and rocking rotation are also predicted for the three-sided culverts, but the bottom slab influence decreases with increasing burial depth and foundation width. The bottom slab combined with the burial depth and structural stiffness also significantly influences the magnitude and distribution of the dynamic earth pressure. The findings of this work shed light on the critical role of the bottom slab in the seismic responses of box culverts and may have a certain reference value for the preliminary seismic design using R-F relation.

**Keywords:** box culvert; earthquake; numerical model; flexibility ratio

## 1. Introduction

For underground structures (e.g., tunnels, subways, culverts, etc.) built in seismically active regions, an appropriate seismic design is of high importance in addition to meet the static design loads. In the past, the seismic design of underground structures has received considerably less attention than other structures at the surface, perhaps because they experienced a lower rate of damages (Hashash *et al.* 2001, Sharma and Judd 1991, Sun *et al.* 2016, Wang *et al.* 2001).

The geometrical feature (e.g., shape, dimensions, depth, etc.) is one of the major factors influencing the seismic damages to underground structures. For the seismic design, the rectangular underground structures have some unique response characteristics that are different from those of circular or horseshoe ones due to the specific geometrical features and construction methods (Cilingir and Madabhushi 2011, Do *et al.* 2014a, b, Golpasand *et al.* 2018, Li and Yang 2019, Liu *et al.* 2018, Wang 1993, Yang and Huang 2011, Yang and Wang 2011). Firstly, the rectangular underground structures are generally built at relatively shallow depths in soils where the ground deformations and the shaking intensities tend to be greater due to the lower stiffness of the backfill soils and the site amplification effect. Secondly, the dimensions of



Fig. 1 Four- and three-sided box culverts

rectangular underground structures are in general larger with some columns, slabs, and walls inside or diaphragm walls outside (e.g., subway station). Dynamic forces will be superimposed on the existing static loads resulting in non-uniform load distributions and significant stress concentrations at some positions (e.g., top and bottom corners). Furthermore, the soil-structure interaction effect becomes more complex and important since the larger structural stiffness, larger dimensions, and increased ground deformations.

In engineering, three- and four-sided box culverts (Fig. 1) are commonly used for a wide range of applications. Although single-cell or multi-cell rectangular structures are rather simple structures, the loading applied to these structures during their construction and subsequent service life can be complex. The stress redistribution of surrounding soils occurs and thus influences the load that acts on the culverts. This is related to the installation methods, the soil conditions, the geometry and stiffness of

\*Corresponding author, Ph.D. Student  
E-mail: sun\_ease@126.com

the structure, and its burial depth (Acharya *et al.* 2016a, b, Kim and Yoo 2005). In recent years, many efforts in the seismic performance of underground structures against ground shaking and earthquake-induced ground failure have been made, to clarify the seismic behavior and to provide guidelines to the rational seismic design. However, compared to circular tunnels (Bilotta *et al.* 2014, Do *et al.* 2015, Fabozzi *et al.* 2018, Shahrouz *et al.* 2010, Sun and Dias 2019a, b, Sun *et al.* 2019, 2020, Zhang *et al.* 2017, 2020), less attention was paid to the rectangular underground structures, particularly with special geometrical features (Wang 2011).

Better understanding the critical response characteristics of box culverts with diverse geometrical configurations under seismic excitations is fundamental to develop a reasonable design method. To date, the issues associated with the culvert seismic behaviour are still not well understood. To gain insights on the critical differences in the seismic performances between three- and four-sided box culverts under ground shaking, this study performs a numerical parametric analysis on diverse soil-culvert systems. Two-dimensional numerical models consider a variety of burial depths, foundation widths and flexibility ratios, assuming a visco-elastic soil condition. The response characteristics are compared in terms of accelerations, Arias intensity, racking deformations, rocking rotations, and dynamic earth pressures. Based on the comparative study performed, the critical role of the bottom slab in the seismic performance of culverts will be highlighted.

## 2. Literature review

This section begins with a brief summarization of the damages to rectangular underground structures in historical earthquakes. Following that, the progress in the simplified seismic design method (i.e., *R-F* method) for rectangular underground structures is presented in section 2.2. In section 2.3, some recent numerical and experimental works on the seismic response of rectangular underground structures in dry soils are presented.

### 2.1 Seismic damages to rectangular underground structures

Severe damages to the rectangular underground structures were rarely reported compared to the ones to the circular- and horseshoe-shaped underground structures. Owen and Scholl (1981) summarized the general characteristics of damages to cut-and-cover conduits and culverts during the 1971 San Fernando earthquake. The general damage patterns were the failure of longitudinal joints, longitudinal cracks and concrete spalling, and plastic hinges at the top and bottom of slabs. They concluded that these damages were probably caused by the significant increase of the lateral forces from the surrounding backfill soil and the long ground motion duration. The Bay Area Rapid Transit system (immersed tube tunnel) which was the first underground structures to be designed with seismic considerations behaved well during the 1989 Loma Prieta earthquake (Hashash *et al.* 2001). Nevertheless, the

situation has been changed in the 1995 Hyogoken-Nambu earthquake. Several large subway stations were heavily damaged in this earthquake and the collapse of the Daikai subway station was the worst one (Iidai *et al.* 1996). The failure mechanism of this station has been extensively studied (An *et al.* 1997, Hashash *et al.* 2001, Huo *et al.* 2005, Parra-Montesinos *et al.* 2006), which could be attributed to:

- The destructive horizontal shear forces on the central columns caused by the relative displacements between the base and ceiling;
- The large axial forces caused by the high level of vertical acceleration, combined with the shear forces led to the brittle shear failure of columns;
- An additional inertial force resulted from the overburden soil;
- The small distance between the sheet pile wall and the station sidewall made the backfill soil compaction difficult, thus the structure could not mobilize passive earth pressures.

Youd and Beckman (1996) summarized the seismic performance of box culverts during past earthquakes and found that most of the damages were concentrated at the construction joints and wall-to-ceiling joints. The seismic damages were due mainly to large inertial forces and permanent ground deformations caused by the soil liquefaction, lateral spreading, and surface rupture. In the following twenty years, damages to large rectangular underground structures were scarcely reported even during the 1999 Chi-Chi earthquake ( $M_L=7.6$ ) and the 2008 Wenchuan earthquake ( $M_L=8.0$ ), despite severe damages to horseshoe-shaped mountain tunnels were reported (Wang *et al.* 2001, Yu *et al.* 2016).

### 2.2 *R-F* method

Underground structures are constrained by the surrounding medium, so they are more sensitive to the earthquake-induced ground deformations. The racking effect on rectangular tunnels caused by ground deformation is the principal types of deformations in the transverse direction, due to vertically propagating seismic waves (Wang 1993). Unlike the circular tunnels, the closed-form solutions (Bobet 2010, Penzien 2000), which permit to directly estimate seismic design loads in the tunnel lining are not available for rectangular underground structures. The so-called free-field racking method (i.e., *R-F* method), which relates the soil free-field distortion deformation to the structure distortion deformation, is generally used for rectangular geometries.

Wang (1993) was the first to propose the free-field racking method accounting for soil-structure interaction. The racking ratios (*R*) for several flexibility ratios (*F*) were deduced using a total number of 36 dynamic finite element analyses. Succeeding to the Wang's study, Penzien and Wu (1998), and Penzien (2000) analytically presented the ratio of *R* as a function of the *F* ratio and Poisson's ratio of soil ( $\nu_s$ ) in an elastic condition. Huo *et al.* (2006) developed a closed-form solution of the racking deformation for deep rectangular underground structures considering the relative stiffness between the soil and the structure, and the aspect

ratios. This solution neglected the contribution of the normal stresses on the deformations, but the soil nonlinearity was introduced by incorporating soil stiffness degradation (Bobet *et al.* 2008). Anderson *et al.* (2008) proposed a closed-form solution similar to Penzien's solution with a constant soil Poisson's ratio (i.e., 0.5), disregarding the  $v_s$  influence.

Generally,  $R-F$  relations assume a perfect adherence to the soil-structure interface. Penzien (2000) provided the only  $R-F$  relation for the full-slip condition. Recently, several numerical works have been performed to investigate the  $R-F$  relation of rectangular underground structures in a wide range of scenarios. Wang (2011) concluded that ground motions with a sharp velocity pulse increased the racking deformation of buried structures. Debiasi *et al.* (2013) conducted numerical parametric analyses to investigate the influence of the soil-tunnel interface (SSI) and aspect ratio on the seismic racking deformation of rectangular tunnels and culverts. They concluded that the SSI effects on the racking deformation vanished as the burial depth increased. Tsiniadis (2017) numerically proposed a series of  $R-F$  relations in a wide variety of scenarios, e.g., soil-tunnel interface condition, single-/multi-cell, dimensions, and burial depths of the tunnel section, soil deposit characteristics, and input motion characteristics. The proposed  $R-F$  relation was then improved by eliminating the rocking response on the actual racking deformation in their subsequent work (Tsiniadis and Pitilakis 2018).

### 2.3 Soil-rectangular underground structure seismic interaction

Cilingir and Madabushi (2011) investigated the burial depth effect on the seismic performance of a square tunnel using centrifuge tests and numerical simulations. They found that square tunnels altered the soil acceleration response according to the structural stiffness and burial depth. They also concluded that deeper tunnels experienced larger dynamic earth pressures but the differences between the deformations of shallow and deep tunnels were negligible. Moss and Crosariol (2013) used shaking table tests to investigate the soil-structure interaction between soft clay and a stiff rectangular tunnel. They suggested that the simplified design methods (Anderson *et al.* 2008) overestimated the racking distortions in soft soil/stiff structure conditions. Ulgen *et al.* (2015a, b) used horizontal extensometers in dynamic centrifuge tests to directly measure the racking deformation of the relatively flexible box structure. Besides, they concluded that the normalized dynamic earth pressure coefficient ( $k_d$ ) decreased as the flexibility ratio increased. A similar relation between the coefficient  $k_d$  and flexibility ratio  $F$  was reported in the numerical study performed by Ertugrul (2016). In the study, the possible explanations for the overestimation of the racking ratios calculated by the Penzien (2000) approach in comparison with numerical predictions and centrifuge tests (Ulgen *et al.* 2015a, b) were presented. Abuhajar *et al.* (2015) performed centrifuge tests and numerical analyses to evaluate the seismic bending moments of a box culvert accounting for the earthquake intensity and frequency,

height of soil cover, and culvert thickness. It was found that the seismic bending moments increased with the increasing input motions intensity, burial depth, and thickness of the culvert.

Tsindis *et al.* (2015, 2016a, b) conducted a series of centrifuge tests and numerical simulations on the dynamic response of square tunnels, focusing mainly on the soil and tunnel relative stiffness, soil-tunnel interface condition, soil nonlinearity, and burial depth. They concluded that the numerical predictions considering a full-slip condition matched well with the experimental data for shallow tunnel while good comparison appeared in the no-slip condition for a deep tunnel. In general, the no-slip interface condition predicted larger dynamic internal forces particularly for the axial force at the corners. The soil nonlinearity, separation, and slippage along the soil-tunnel interface affected the surrounding soil yielding thus led to the complex distribution and magnitude of the dynamic earth pressures. A poor comparison between simplified design methods and dynamic analysis and experimental data was presented, especially for the flexible tunnel in nonlinear soils.

Hushmand *et al.* (2016a, b, c) conducted a series of centrifuge experiments to evaluate the seismic performance of underground reservoir structures (with rectangular cross-section) accounting for the structural stiffness, backfill soil type and slope, fixity conditions, and ground motion characteristics. They concluded that underground reservoir structures were not completely rigid and could deform or rotate based on the stiffness, site conditions, and ground motion characteristics. The underground structures experienced notable dynamic earth pressures ( $\Delta\sigma_E$ ) as they increased linearly with the depth for a shallow flexible structure. While for stiff structures,  $\Delta\sigma_E$  followed a three-order polynomial distribution. However, none of the available simplified methods derived for the retaining walls could precisely capture the actual distribution and magnitude of  $\Delta\sigma_E$  along the sidewall due to the kinematic constraint at their top and bottom slab. In lie with the study of Cilingir and Madabushi (2011), the buried structure also was found to alter the acceleration response because of the kinematic interaction. The amplification effect was more evident near the top corner of shallow flexible structures whereas the added cover, stiffness of the backfill soil, and increased shaking level slightly reduced the amplification effect. The results suggested that the Anderson *et al.* (2008) method underestimated the racking deformations of stiff structures while slightly overestimated the racking deformation of flexible structures. In the companion numerical studies, Deng *et al.* (2016) evaluated the capabilities of an advanced constitutive model (i.e., PDMY02) coupled with various modulus reduction curves on the seismic response of relatively stiff reservoir structure. They found that considering the upper Darendeli modulus curve in the numerical predictions permitted to obtain a good agreement with the centrifuge results. Using the domain reduction method combined with the equivalent linear soil model, Seylabi *et al.* (2018) illustrated that the mismatches between the numerical simulations and centrifuge tests for the dynamic earth pressures could be attributed to the local nonlinearities of soil and reservoir structures contact that cannot be captured in the numerical model.

In summary, despite many efforts that have been made

for understanding the seismic behaviour of rectangular underground structures, some significant disparities exist in the academia and engineering practices (Hashash *et al.* 2001, Sun *et al.* 2016). Besides, few studies have been conducted on the seismic response of three-sided box culverts, and the differences in the seismic performance between the three- and four-sided box culverts are not well understood. The important open issues regarding the bottom slab effect in the seismic behaviour of box culverts need further investigation, which will benefit the practical seismic design.

### 3. Numerical model

#### 3.1 Outline of the problem

The problem investigated here is schematically illustrated in Fig. 2. A concrete box culvert embedded in a homogeneous soil deposit at 30 m depth, resting on the elastic bedrock is considered. To highlight the effect of the bottom slab on the seismic response of the culvert, three- and four-sided culverts are modeled, respectively.

The studied box culverts have a width ( $W$ ) of 4 m and height ( $H$ ) of 3.5 m corresponding to an aspect ratio equals to 1.14. This is the most common size of culvert used in engineering practice (Acharya *et al.* 2016b). It is worth noticing that culverts with large dimensions generally need a central column or wall at the middle of the span to satisfy design loads under static conditions, but such a configuration is not common for three-sided box culverts. Particularly, three-sided box culverts are generally supported on continuous spread foundations or pile-supported footings. The width of strip foundation ( $W_f$ ), varies from 0 to 3 m, is considered for reality.

The burial depth of culverts ( $h$ ), varies from 1 to 10 m, to compare the seismic response of shallow and deep culverts. The thickness of both the slab and sidewall ( $t$ ), is assumed to be the same but with varying values (i.e.,  $t=0.2, 0.3, 0.418, 0.6$  m), to investigate the response of rigid and flexible culverts. The soil-culvert relative stiffness is evaluated by the flexibility ratio  $F$ , which can be calculated with the following equation (Wang 1993):

$$F = (G \times W)/(S \times H) \quad (1)$$

where  $G$  is the soil shear modulus and  $S$  is the required concentrated force to cause a unit racking deflection of the culvert. The small thickness of the structure induces a large flexibility ratio and the ratio of  $F$  varies from 0.35 (i.e. rigid culvert) to 9.4 (i.e.. flexible culvert) in this study. It is worth noticing that the calculated flexibility ratio corresponds to the four-sided culvert because the analytical solution for the three-sided culvert is unavailable.

#### 3.2 Numerical analysis

Numerical parametric analyses are carried out under plane strain conditions, using the two-dimensional finite difference code *FLAC* version 7.0 (Itasca 2011). The dimensions of the numerical model are the following ones: height of 30 m and width of 100 m, as shown in Fig. 3. The

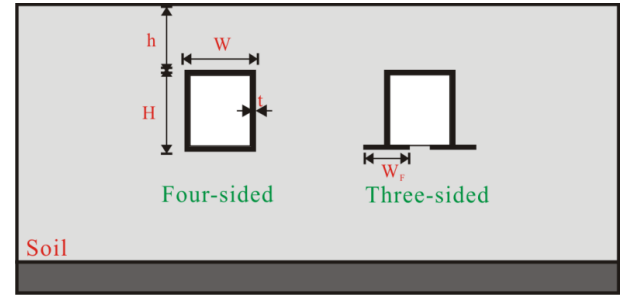


Fig. 2 Schematic representation of the culvert configuration

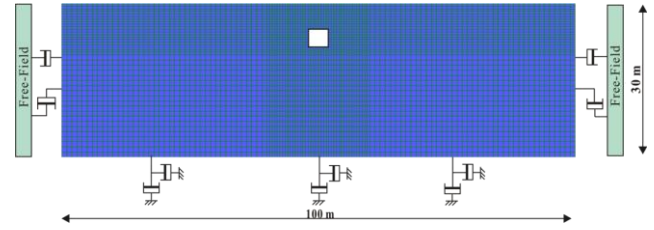


Fig. 3 Numerical model ( $h=5$  m)

model width is determined according to sensitivity analysis to eliminate the effect of the lateral boundaries on the numerical predictions.

To avoid the complexity of a fully nonlinear dynamic analysis and to reduce the uncertainty in the numerical predictions caused by the selection of constitutive models of materials (Yang and Yin 2005, 2010), both the culvert and soil are assumed to be linear elastic. The soil properties are as follows: density  $\rho_s=1900$  kg/m<sup>3</sup>, shear wave velocity  $V_s=150$  m/s, and Poisson's ratio  $\nu_s=0.3$ ; while the parameters of the culvert are: density  $\rho_f=2500$  kg/m<sup>3</sup>, elastic modulus  $E_f=30$  GPa, Poisson's ratio  $\nu_f=0.25$ . These parameters of soil and culvert are taken from the literature and correspond to real values in practice (Sun and Dias, 2019a; Tsinidis *et al.* 2016). The soil-culvert interaction is assumed as a perfect bonding, disregarding the separation and slippage between the soil and culvert in this study. These considerations permit to consider the most unfavorable internal forces and racking deformations scenarios (Tsinidis 2017). The effects of soil nonlinearity and soil-structure interface slippage on the seismic response of underground structures were well investigated in the previous studies (Sun and Dias 2019a, b, Tsinidis *et al.* 2015, 2016a, b).

Another important issue associated with modeling a three-sided culvert is the fixity condition between the sidewall and foundation. Limited to the two-dimensional numerical model used in this work, rotation, and separation between the sidewall and foundation cannot be accurately described. However, based on the study of the pile-cap connection (Sadek and Shahrour 2006), it can speculate that the calculated results of three-sided culverts with a foundation width of 0 m should be the response upper limit since the sidewall deforms freely with no kinematic constraint comes from the foundation. In this study, the sidewall directly connects to a foundation is considered.

Before the seismic analysis, a static analysis is conducted to determine the initial state of stresses around the culverts. For the static analysis, the gravity load is

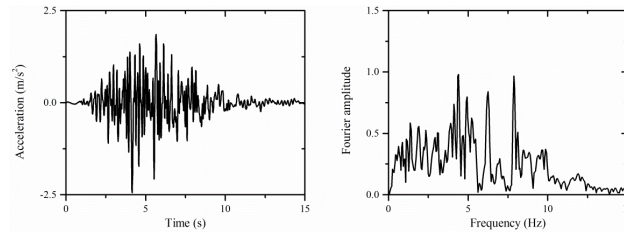


Fig. 4 Acceleration time history and Fourier amplitude spectrum of the Nice wave

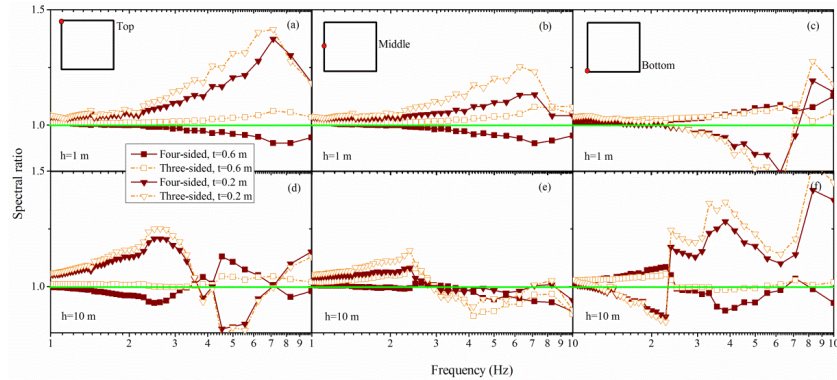


Fig. 5 Spectra ratio (5% damped) of the culvert to free-field accelerations at the top, middle and bottom positions of the sidewall

applied. The displacements in two directions along the model base and horizontal displacements along the lateral sides are fixed. The culvert excavation is simulated in one step with a “null” model. In the subsequent seismic analysis, the free-field boundaries are applied along the lateral sides to properly absorb the outward waves while a quiet boundary is applied at the model base to simulate the elastic bedrock. The Nice ground motion is selected as the seismic input after a high frequency cutoff and baseline correction, as plotted in Fig. 4. The acceleration time history (with an amplitude of  $1.25 \text{ m/s}^2$ ) is integrated into the velocity time-history, then transformed into a shear stress time-history. It is applied at the model base considering the vertically propagating of the ground motion.

The maximum mesh size employed in the numerical model is equal to 1.0 m, based on the well-known equations (Kuhlemeyer and Lysmer 1973) while the mesh around the culvert is refined (0.5 m). The Rayleigh type viscous damping is introduced in the dynamic analysis. Since the Rayleigh damping is frequency-dependent thus it may result in an over-damping or an under-damping of the wave propagation (Itasca 2011, Sun and Dias 2018, Sun *et al.* 2019a). According to the study of Kwok *et al.* (2007), the frequency interval could be determined by the 1<sup>st</sup> and 3<sup>rd</sup> mode frequency of the soil deposit which corresponds to a center frequency is of 2.8 Hz in this study. A minimum damping ratio of 1.0% is adopted which is adequate to remove the possible high frequency noise and avoid low-level oscillations.

## 4. Numerical results

### 4.1 Accelerations

The influences of the bottom slab on the acceleration

responses in terms of the spectral ratios and normalized Arias intensity for different burial depths and flexibility ratios are investigated in this subsection. The spectral ratio is defined as the ratio of the spectral acceleration measured on the left sidewall to those in the far-field at the corresponding elevation. Fig. 5 shows the spectral ratios at the top, middle and bottom positions in the case of burial depth  $h=1$  and 10 m, corresponding to the thickness  $t=0.2$  and 0.6 m for both three- and four-sided culverts. Similar results observed in other thicknesses are not presented for clarity.

The presence of the culvert alters the acceleration response at different elevations compared to the free-field ones due mainly to the kinematic interaction. The amplification or de-amplification effect relates to the burial depth, the thickness of the culvert, and the bottom slab. The maximum spectral ratio is generally observed for the flexible culvert (e.g.,  $t=0.2$  m). An additional increase in the spectral ratio is observed for the three-sided culvert due to the lower deformation constraint. No obvious change is reported in acceleration records on the three-sided culvert with a thickness of 0.6 m (i.e., a spectral ratio of around 1.0) because a pure shear state appears (will be plotted in Fig. 8), meaning that the culvert deforms closely the same with the surrounding soil.

For the shallow culvert (e.g.,  $h=1$  m), the spectral ratio is increased from the bottom to the top corner, with a maximum amplification ratio of 1.4. As the burial depth increases, the spectral ratio tends to decrease except for  $t=0.2$  m at the bottom (Fig. 5(f)). This could be attributed to the movement of the culvert is more controlled by the surrounding soil with the increasing confining pressure (i.e., burial depth), thus reducing the amplification effect (Hushmand *et al.* 2016a, b). The larger spectral ratio observed in Fig. 5(f) could be attributed to the greater

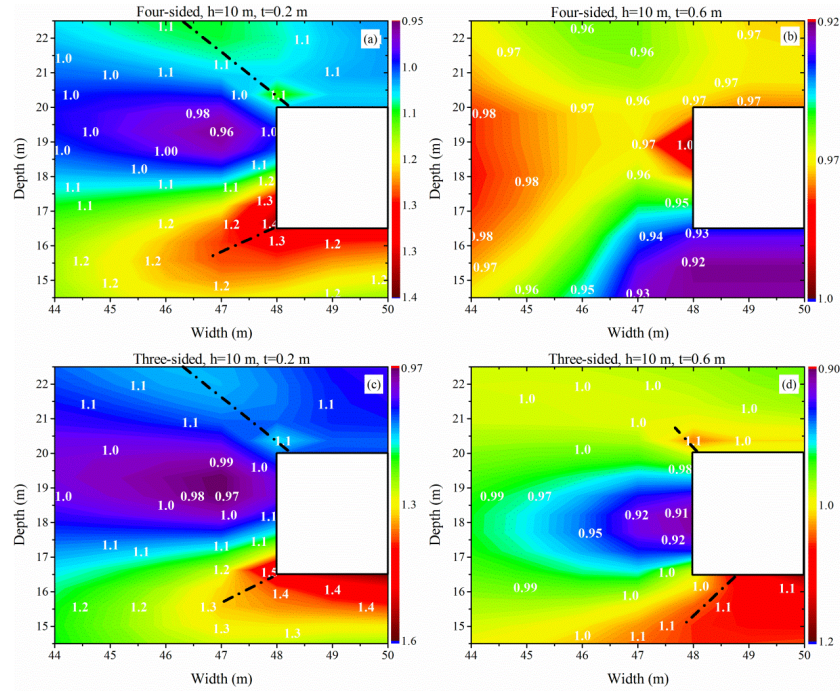


Fig. 6 Arias intensity amplification ratio around three- and four-sided culverts with a thickness of 0.2 and 0.6 m in a shallow depth ( $h=1$  m)

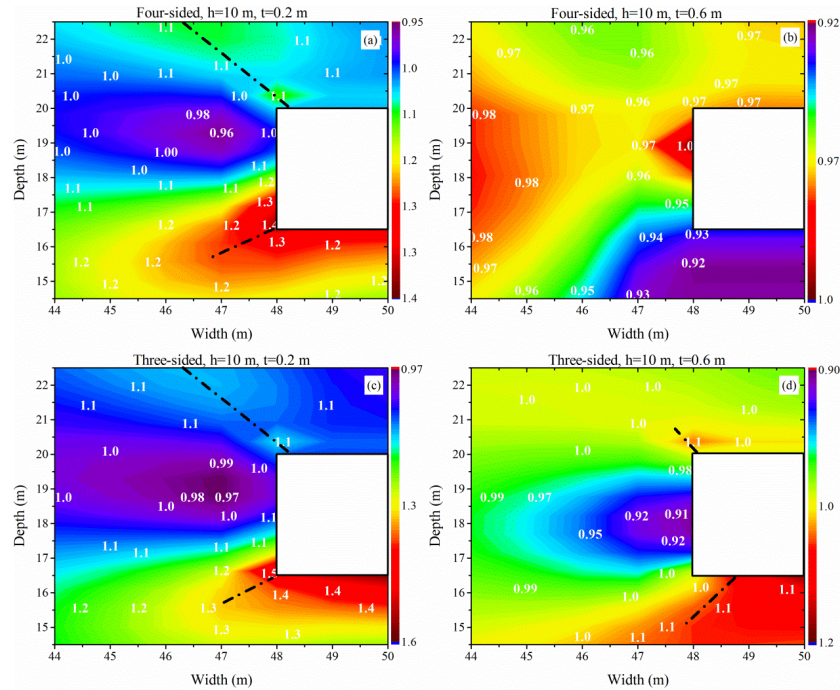


Fig. 7 Arias intensity amplification ratio around three- and four-sided culverts with a thickness of 0.2 and 0.6 m in a deep depth ( $h=10$  m)

relative movement of the more flexible culvert with respect to the surrounding soil, under both the static and dynamic loads. Another observation from Fig. 5 is that the frequency at which the spectral ratio reaches the maximum value tends to reduce as the burial depth increases. It is probably due to the reflected wave with high frequency trapped in the soil portion between the culvert and the ground surface at a shallow depth (Lancioni *et al.* 2014).

To compare the energy accumulated around the culvert, the accumulative energy can be evaluated by the Arias intensity of the acceleration time history. The normalized accumulative energy,  $I_{A, norm}$ , is calculated using the following formula (Cilingir and Madabhushi 2011):

$$I_{A, norm} = \frac{\int_0^{T_d} a_{culvert}(t)^2 dt}{\int_0^{T_d} a_{free-field}(t)^2 dt} \quad (2)$$

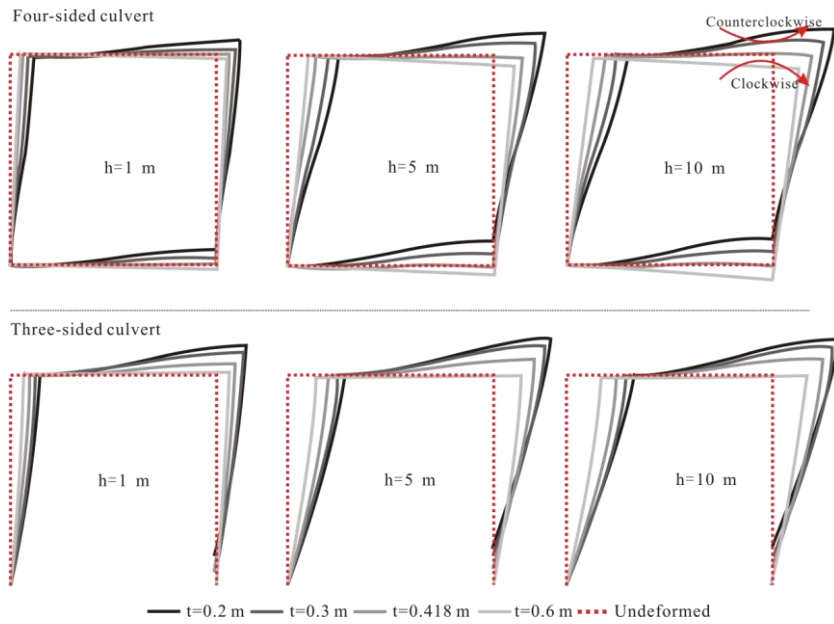


Fig. 8 Dynamic deformed shapes of three- and four-sided culverts at the time step of the maximum racking deformation (magnification: 300)

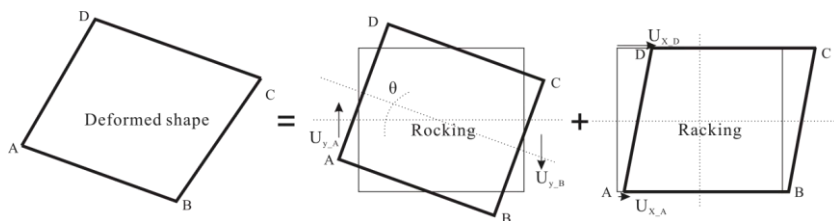


Fig. 9 Definition of the racking deformation and rocking rotation

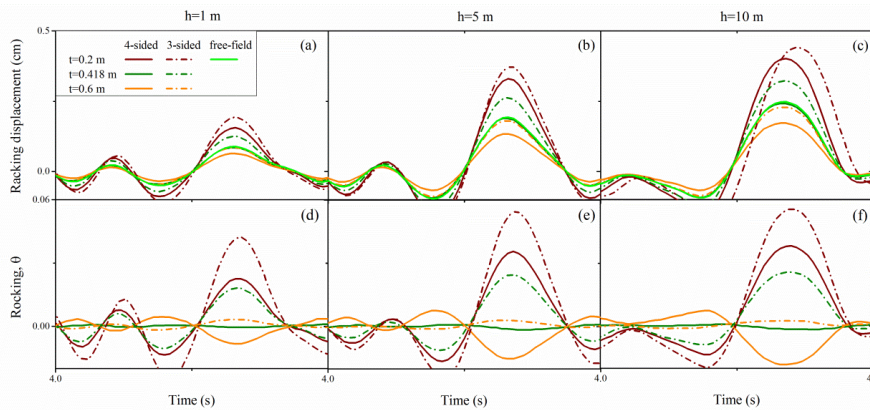


Fig. 10 Racking deformation and rocking rotation time histories of three- and four-sided culverts for various thicknesses ( $t=0.2, 0.418$  and  $0.6$  m) and depths ( $h=1, 5$  and  $10$  m)

where  $a_{culvert}(t)$  and  $a_{free-field}(t)$  are respectively the acceleration time histories of the culvert and free-field cases at the same point and  $T_d$  is the ground motion duration. The representative distributions of the values of  $I_{A\_norm}$  for the three- and four-sided culverts, corresponding to  $h=1$  and  $10$  m,  $t=0.2$  and  $0.6$  m are respectively showed in Figs. 6 and 7.

For shallow flexible culverts (Figs. 6(a) and 6(c)), the accumulative energy is amplified near the top corner of the culvert, while three-sided culverts tend to strengthen such an amplification effect. The position of the maximum

amplification appears depends on the complex wave-culvert-soil interaction, which in good agreement with the findings of Sun *et al.* (2019). As the thickness increases, the reduced value of  $I_{A\_norm}$  occurs at the top of the culvert. It means that the rigid culvert represents an obstacle, which obstructs the wave propagation. An insignificant amplification ( $\sim 1.1$ ) observed at the bottom corner for  $t=0.6$  m (Figs. 6(b) and 6(d)) because of the slight increase in the spectral ratio in the investigated frequency range (Fig. 5). For deep culverts, a considerable amplification occurs

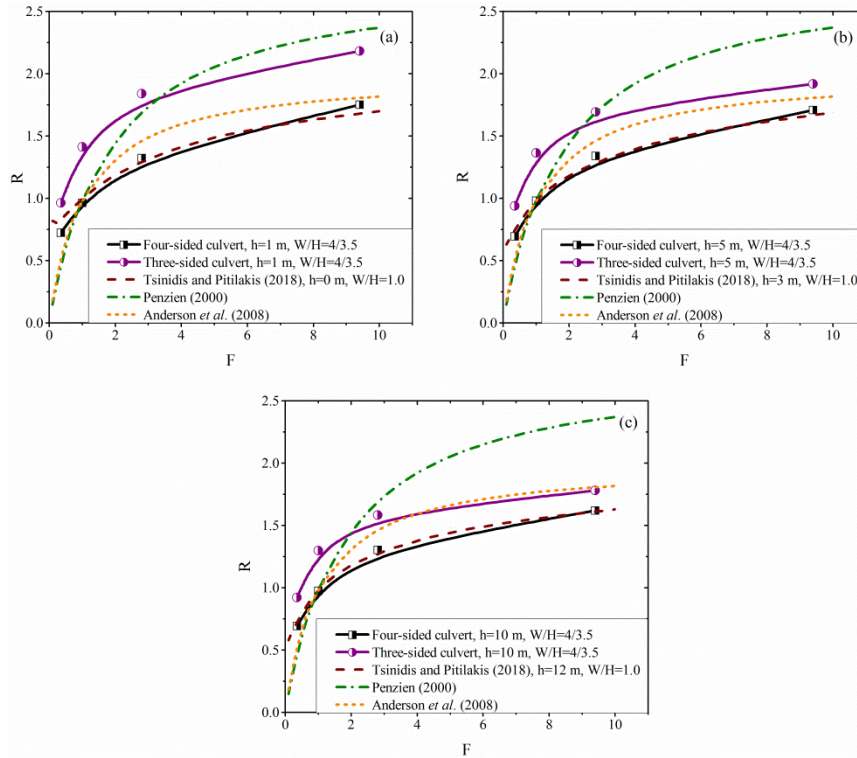


Fig. 11 Racking ratios versus flexibility ratios of three- and four-sided culverts for three burial depths

around the bottom corner of flexible culverts (Fig. 7(a) and 7(c)). Similarly, the amplification on the normalized accumulative energy is also more evident for three-sided culverts and tends to decrease with increasing culvert thickness (Fig. 7(b) and 7(d)).

As a summary, the three-sided culvert has a more pronounced amplification influence on the spectral acceleration and Arias intensity than four-sided culvert, which is related to the burial depth and structural stiffness. The presence of the bottom slab surely increases the overall stiffness of culvert and considerably modifies the soil-culvert interaction. As illustrated in Fig. 5, this dynamic interaction is also related to the ratio between culvert dimension and wavelength: wave with large wavelength (low frequency) propagates practically undisturbed, both three- and four-sided culvert represents ignorable perturbation (i.e., a spectral ratio of near 1.0).

#### 4.2 Deformations and rotations

The influence of the bottom slab on the culvert deformation response is an important issue since the deformation-based seismic design is gradually being accepted in the preliminary practical design (Hashash *et al.* 2001; Sun and Dias, 2019). The deformation response characteristic of three- and four-sided culverts for different thicknesses and burial depths are investigated in this section. Fig. 8 presents the typical deformed shapes of the three- and four-sided culverts during shaking computed at the time step of the structure maximum racking distortion.

The complex racking-rocking responses are observed in all the examined cases. For both three- and four-sided culverts, the racking deformations increase with the

decrease of the thickness. Besides, the inward-outward deformations of the sidewalls and slabs, coupled with counterclockwise rocking rotations appear for the flexible culvert (e.g.,  $t=0.2$  and  $0.3$  m) because of their low resistance to the deformation of the surrounding soil. The four-sided culvert with a thickness  $t=0.418$  m corresponds to a flexibility ratio  $F=1.0$ , illustrating that the culvert is subjected to a pure shear state and the culvert deforms the same with the surrounding soils. Further increasing the thickness (e.g.,  $t=0.6$  m) results in a clockwise rocking rotation, which is contrary to the flexible culvert case. Although the flexibility ratio of the three-sided culvert cannot be given precisely, it can be suspected that a three-sided culvert will have a higher flexibility ratio due to the lack of the kinematic constraint at the bottom slab. As a result, a three-sided culvert with a thickness of  $0.418$  m behaves more flexibly while culvert with a thickness of  $0.6$  m is more or less corresponding to a pure shear state.

As stated in section 2.2, the  $R$ - $F$  method is generally used for the preliminary design of rectangular underground structures. Racking ratio  $R$  is defined as the ratio of the structural racking deformation ( $\Delta_{str}$ ) and soil deformation ( $\Delta_{ff}$ ) in the free-field case at the same elevation (Wang, 1993):

$$R = \Delta_{str} / \Delta_{ff} = (U_{X_D}(t) - U_{X_A}(t))_{str} / (U_{X_D}(t) - U_{X_A}(t))_{ff} \quad (3)$$

where  $U_{X_D}(t)$  and  $U_{X_A}(t)$  are respectively the computed horizontal displacement time histories at the top corner (position D) and bottom corner (position A) (Fig. 9). To quantify the rocking response of rectangular culverts mobilized during ground shaking, an average rotation of the

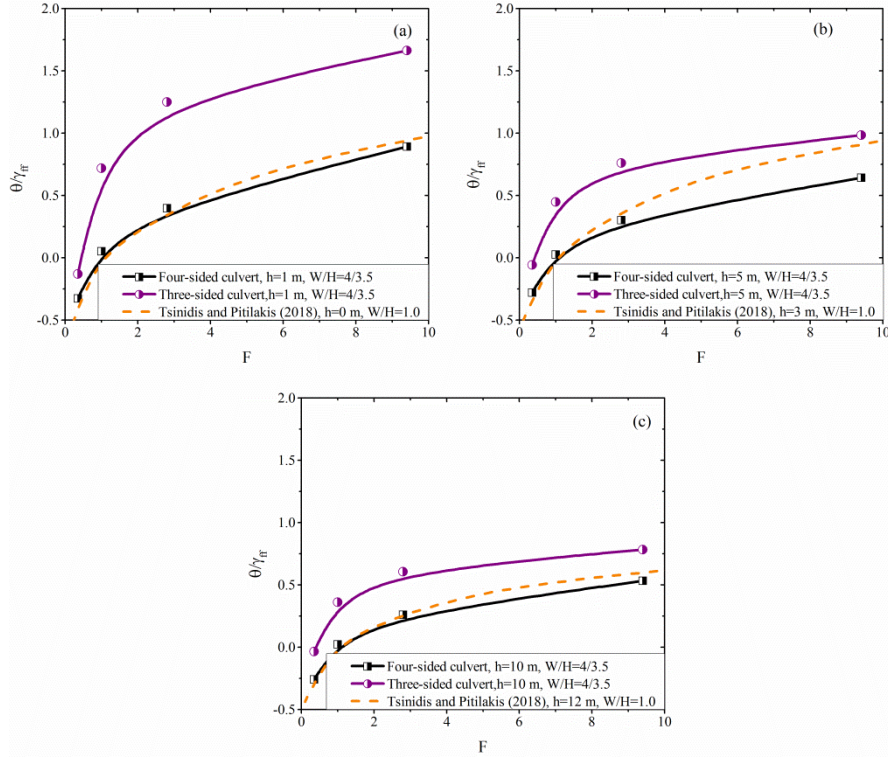
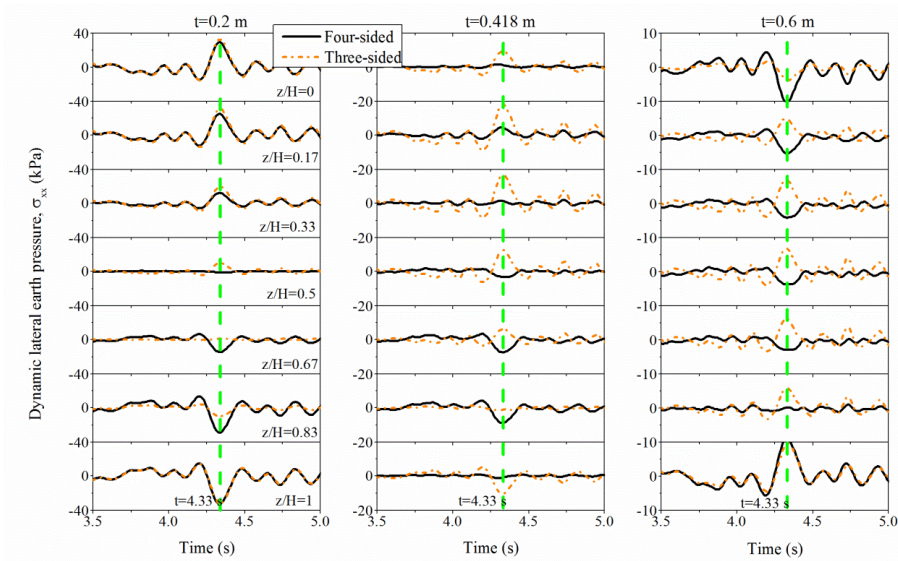


Fig. 12 Normalized rocking rotations versus flexibility ratios of three- and four-sided culverts in three depths


 Fig. 13 Dynamic earth pressure time histories of three- and four-sided culverts with three thicknesses ( $h=5$  m)

culvert  $\theta$  is defined (Tsinidis 2017):

$$\theta = \max\{\tan^{-1}[(U_{Y_A}(t) - U_{Y_B}(t))/W]\} \approx \max[(U_{Y_A}(t) - U_{Y_B}(t))/W] \quad (4)$$

where  $U_{Y_A}(t)$  and  $U_{Y_B}(t)$  are the computed vertical displacement time histories at positions A and B (Fig. 9),  $W$  is the culvert width.

The representative time histories of  $\Delta_{str}$ ,  $\Delta_{ff}$ , and  $\theta$  during the ground shaking are respectively presented in Fig. 10. Only the responses in the time interval from 4.0 to 4.5 s including the maximum value are shown for clarity. Both

the racking deformations and rocking responses are generally increased with increasing burial depth in this work. The maximum response is reported in the flexible three-sided culvert (e.g.,  $t=0.2$  m). The four-sided culvert with a thickness of 0.428 m and the three-sided culvert with a thickness of 0.6 m capture the same racking deformation with the free-field meanwhile the corresponding rocking rotation closes to zero, indicating a pure shear state. Contrary to the racking deformation, the positive correlation between the rocking rotation and the structural stiffness is only established for flexible culverts. Larger rocking rotation is observed for the flexible three-sided culvert at a

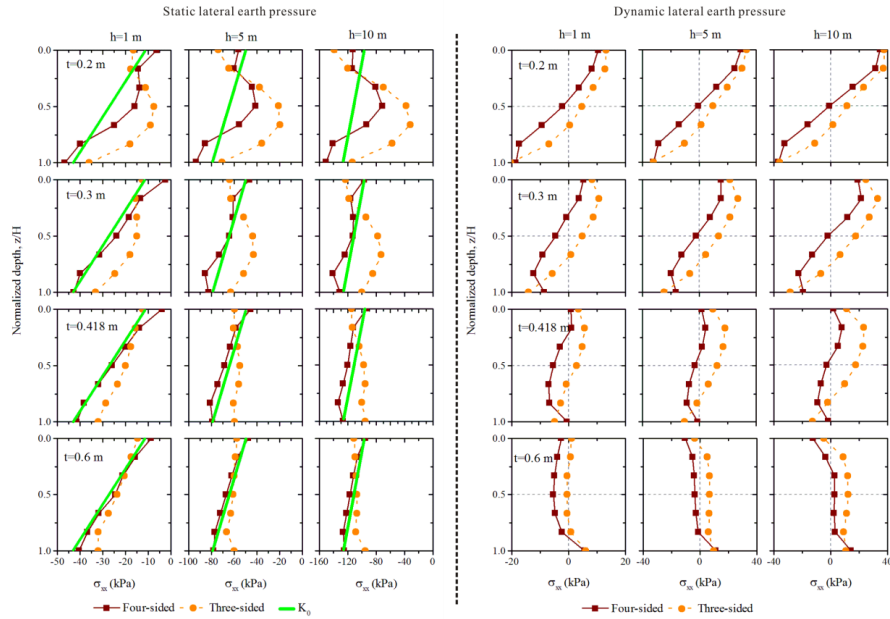


Fig. 14 Distribution of the static earth pressures (left) and the dynamic earth pressures (right) of three- and four-sided culverts for different thicknesses and depths

deep depth. However, the rigid culvert also rotates more but in the opposite direction as the flexible culvert. It highlights that soil culvert relative stiffness governs both the amplitude and direction of the rocking rotation.

Fig. 11 compares the racking ratio versus the flexibility ratio of the three- and four-sided culverts. The  $R$ - $F$  relations computed by Anderson *et al.* (2008), Penzien (2000), and Tsinidis and Pitilakis (2018) are also presented. It should be noticed that the flexibility ratio, is calculated based on Eq. (1) for the four-sided culverts and the same  $F$  ratio is approximately adopted for three-sided culverts to compare with the existing results.

The racking ratios of all the examined cases increase with the increasing flexibility ratio, with the larger ratios appear in the three-sided culvert at a shallow depth. It illustrates that the deformation of the surrounding soils is gradually controlling the culvert racking deformation as the burial depth increases. The difference between the racking ratios for the three- and four-sided culverts is relatively small for the very rigid (e.g.,  $F=0.35$ ) and very flexible (e.g.,  $F=9.4$ ) culvert, particularly at a deep depth. This is because the presence of the bottom slab has a relatively small contribution to the overall stiffness of culvert in these two scenarios. Further, it can be speculated that the three- and four-sided culverts capture the same racking ratio for the extremely rigid (e.g.,  $F=0$ ) or extremely flexible culverts (e.g.,  $F=\infty$ ). Compared to previous studies, the racking ratios of four-sided culverts in this study agree very well with the results of Tsinidis and Pitilakis (2018). However, both the Anderson *et al.* (2008) and Penzien (2000) methods tend to underestimate the racking ratios for rigid culverts and overestimate the racking ratios for flexible culverts, particularly for the deeply buried culvert.

Fig. 12 compares the normalized rocking rotations ( $\theta/\gamma_{ff}$ ) versus flexibility ratio ( $F$ ), in which  $\gamma_{ff}$  is the maximum shear strain of the far-field at the corresponding elevation. The  $\theta/\gamma_{ff}$ - $F$  relation calculated by Tsinidis and Pitilakis

(2018) is also presented. The physical meaning of negative  $\theta/\gamma_{ff}$  ratio is the following one: the culvert in these cases rotates in the opposite direction compared to culvert with positive  $\theta/\gamma_{ff}$  ratios (Fig. 10). For rigid culverts (e.g.,  $F<1.0$ ), the  $\theta/\gamma_{ff}$  ratios decrease with the increasing flexibility ratio until  $F=1.0$  where a pure shear state appears for the four-sided culverts ( $\theta/\gamma_{ff}=0$ ). Further increase of the flexibility ratio (e.g.,  $F>1.0$ ) results in a significant increase in the ratio of  $\theta/\gamma_{ff}$ , particularly for the three-sided culverts at a shallow depth. This can be attributed to the fact that culverts experience larger inertial forces and fewer deformation constraints when culverts are shallowly buried. Similar to racking ratios, the relative differences of normalized rocking ratios between the three- and four-sided culverts decrease with increasing burial depth. In comparison with the results of Tsinidis and Pitilakis (2018), a good agreement is observed in the cases of  $h=1$  and 10 m (four-sided culverts). The discrepancy observed in a burial depth of  $h=5$  m for the higher flexibility ratios can be partly explained by the different burial depths and aspect ratios used.

### 4.3 Earth pressures

The typical dynamic earth pressure time histories along the left sidewall are compared in Fig. 13, corresponding to a burial depth of  $h=5$  m and thickness  $t=0.2$ , 0.418, and 0.6 m. The dynamic earth pressure is obtained by subtracting the static earth pressure computed at the end of the culvert excavation from those at the end of the dynamic analysis. The effects of the culvert thickness and presence of the bottom slab on the computed dynamic earth pressures are highlighted.

Generally, the time histories of the dynamic earth pressure on the flexible four-sided culverts (e.g.,  $t=0.2$  m) are in phase with the ones of the flexible three-sided

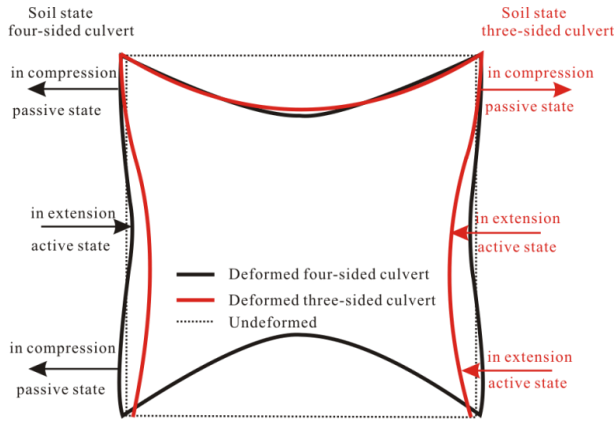


Fig. 15 Deformed shapes of three- and four-sided culverts at the end of the static analysis (magnification: 300,  $h=5$  m)

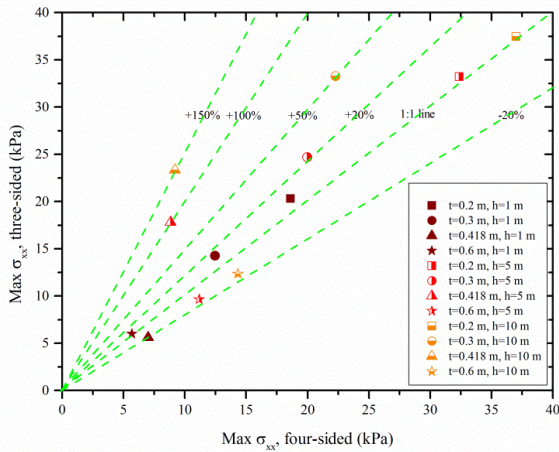


Fig. 16 Comparison of maximum dynamic earth pressures in three- and four-sided culverts

culverts. The out of phase of the dynamic earth pressures in the two types of culverts appear with the increasing thickness (e.g.,  $t=0.6$  m). It illustrates that a different deformation mode exists between three- and four-sided culverts. For a specific culvert, the sign (positive or negative) of the dynamic earth pressures at different locations ( $z/H$ ) is changing. The soil-culvert relative stiffness governs the racking and rocking responses, as stated above, thus resulting in various stress states of the surrounding soil along the sidewall.

Fig. 14 presents the distributions and magnitudes of static (left) and dynamic (right) earth pressures along the left sidewall. The numerically computed static earth pressures are also compared with theoretical ones under at-rest ( $K_0$ ) conditions. The dynamic earth pressure is computed at the time step of the maximum culvert racking deformation.

In the static analysis, the larger static earth pressures are observed around the bottom corners while smaller static earth pressures occur at the sidewall midpoint compared to theoretical ones, particularly for more flexible culverts. This is due to the in-ward deformation of the slabs and sidewalls of the flexible culverts at the end of culvert excavation, as shown in Fig. 15. The increased static earth pressures at two

corners for flexible four-sided culverts (e.g.,  $t=0.2$  m) result from the out-ward deformations around the two corners compress the surrounding soil. It leads to a “passive state” thus increasing the static earth pressures. On the contrary, the decreased static earth pressure in the sidewall midpoint of flexible four-sided culvert could be attributed to the soil around the sidewall midpoint produces an “arching effect” due to the in-ward deformation, resulting in an “active state”. The increase in the static earth pressure at the top corner and decrease in the static earth pressure at the middle is more evident for the three-sided culvert, due to its noticeable out-ward and in-ward deformation respectively. As the thickness increases, the calculated static earth pressures tend to fit well with theoretical ones for the four-sided culverts (e.g.,  $t=0.6$  m) whereas an underestimation of the earth pressures around the bottom corner is always found for the three-sided culverts.

The presence of the bottom slab, combined with the burial depth and culvert thickness significantly influences the distribution and magnitude of the dynamic earth pressures. Concerning the distribution of the dynamic earth pressures, anti-symmetric distributions along the left sidewall are observed for the deeper four-sided culverts (e.g.,  $h=5$  and 10 m). The anti-symmetric response indicates that the upper part of the left sidewall is subjected to active earth pressures, while the lower part is subjected to passive earth pressures. The stiffness of culvert significantly affects the distribution of dynamic earth pressures. With the thickness increases, the shapes of the dynamic earth pressure profiles generally change from triangular to three-order polynomial for the four-sided culverts. This conclusion is in line with the centrifuge results performed by Hushmand *et al.* (2016a). The distributions of the dynamic earth pressures for the three-sided culverts follow a two-order polynomial shape in this study since no peak response is observed close to the bottom corner ( $z/H=0.83$ ).

Concerning the magnitude of the dynamic earth pressure, a positive value means that the total earth pressure decreases compared to the initial static earth pressure (active earth pressure) and a negative value means an increase of the total earth pressure (passive earth pressure). The dynamic earth pressure decreases with the increasing culvert thickness while deeper culverts experience larger dynamic earth pressures (Cilingir and Madabhushi 2011). Compared to four-sided culverts, three-sided culverts predict larger dynamic earth pressures at the upper part of the sidewall. The larger right-ward racking deformation (Fig. 8) leads to the fact that the surrounding soils are in tension states (active earth pressures). While for the lower part of the sidewall, the total earth pressures of four-sided culverts generally increase slightly because the soils are in compression states. For the three-sided culverts, the soil at the lower part of the sidewall changes gradually from tension to compression state, which is strongly related to the burial depth and culvert thickness.

It should be noted that the maximum dynamic earth pressure is not always computed at the corners although the racking deformation of the top corner is maximum (i.e., the higher resistance of the soil to the increased deformations). A slight decrease of the dynamic earth pressure at the top corner is observed in some cases (e.g.,  $t=0.3$  and 0.418 m).

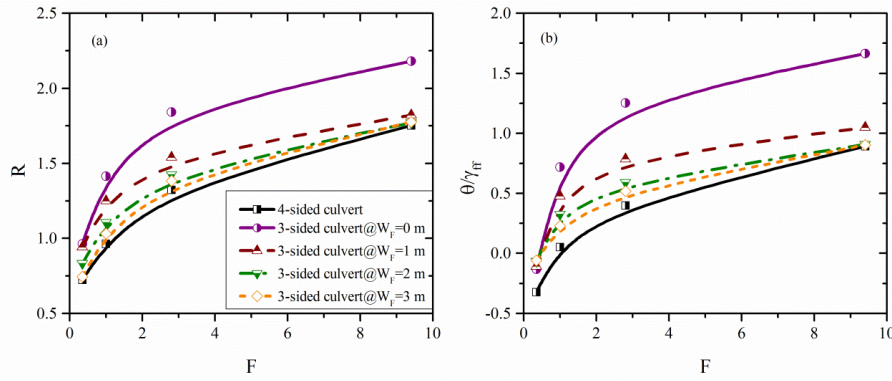


Fig. 17 Racking ratios and normalized rocking rotations for various foundation widths of three-sided culverts

This may be attributed to the local curvature of the sidewalls at these locations caused to maintain the angle of the concrete corner ( $90^\circ$ ). These curvatures are amplified for the three-sided culverts, due to the higher flexibility of the sidewall (Ulgen *et al.* 2015b). Also, the dynamic earth pressures developed at the bottom corners are higher than the top corner ones for shallow culverts, since the overburden soil weight and the associated confinement around the top corners are highly reduced.

Fig. 16 compares the absolute maximum dynamic earth pressures of three- and four-sided culvert. The difference is relatively small (around 20%) for the rigid and very flexible culverts (i.e.,  $t=0.6$  and  $0.2$  m) and shows less sensitivity to the burial depth. However, for culverts with a thickness of  $0.3$  and  $0.418$  m, the difference tends to increase with increasing burial depth. The maximum relative deviation up to 150% is observed for the culvert with a thickness of  $0.418$  m in the case of  $h=10$  m.

## 5. Parametric study on the influence of the foundation width

In practice, three-sided culverts are generally supported on continuous spread foundations. It results in, to some significant degree, the presence of the foundation will affect the overall response of three-sided culverts. To gain insights into the influence of foundation width ( $W_F$ ) on the racking and rocking responses of three-sided culverts, a range of  $W_F$  values, from 0 to 3 m, is investigated in this section with the help of a through parametric analysis. The thickness of the foundation is identical to the thickness of the sidewall and the other parameters adopted in the analysis are the same as the ones used in section 4.

Fig. 17 shows the evolutions of the values of the racking ratios ( $R$ ) and normalized rocking rotations ( $\theta/\gamma_{ff}$ ) with increasing flexibility ratios for different values of  $W_F$ . The corresponding responses of four-sided culverts are also presented in the figure for comparison. The results show that the racking ratios and normalized rocking rotations of the three-sided culvert are considerably decreased with the increasing foundation width. This is because the interaction between the foundation and the surrounding soil limits the overall movement of the three-sided culvert, which develops an additional restraint. Besides, the increased foundation width enhances the overall stiffness of the

Table 1 Relative differences (%) of the calculated ratios of  $R$  and  $\theta/\gamma_{ff}$

| $F$  | $R$   |       |       |         | $\theta/\gamma_{ff}$ |       |       |         |
|------|-------|-------|-------|---------|----------------------|-------|-------|---------|
|      | $W_F$ |       |       | 4-sided | $W_F$                |       |       | 4-sided |
|      | 1 m   | 2 m   | 3 m   |         | 1 m                  | 2 m   | 3 m   |         |
| 0.35 | -2.1  | -13.4 | -22.6 | -24.9   | -17.7                | -50.8 | -54.8 | 147.9   |
| 1.0  | -11.7 | -21.7 | -27.1 | -31.9   | -33.5                | -54.8 | -68.3 | -92.9   |
| 2.8  | -16.4 | -22.7 | -24.9 | -28.2   | -37.2                | -52.8 | -58.6 | -68.1   |
| 9.4  | -16.4 | -18.7 | -18.5 | -19.7   | -37.0                | -45.4 | -45.7 | -46.4   |

culvert thus increases its resistance capacity to deformation of the surrounding soil. Besides, the racking and rocking responses of three-sided culverts become closer to four-sided culvert ones, as the width of the foundation increases. This means that the  $R$ - $F$  and  $\theta/\gamma_{ff}$ - $F$  relations developed for the four-sided culvert can be properly applied as the lower limit for the three-sided culvert.

The relative differences of the calculated ratios of  $R$  and  $\theta/\gamma_{ff}$  to those in the three-sided culvert without foundation are presented in Table 1. The presence of the foundation can effectively reduce the seismic responses of the three-sided culvert, with a maximum reduction of 27.1% in the racking ratios and of 68.3% in the normalized rocking rotations. For the rigid culvert, the reduction effect tends to increase significantly with increasing foundation width while both ratios show less sensitivity to the change in the foundation width for the flexible culvert (e.g.,  $F=9.4$ ). For specific, the  $R$  ratio of the rigid culvert (e.g.,  $F=0.35$ ) is reduced from 0.94 (-2.1%,  $W_F=1.0$  m) to 0.75 (-22.6%,  $W_F=3.0$  m) while the ratio is reduced from 1.82 (-16.4%,  $W_F=1.0$  m) to 1.78 (-18.5%,  $W_F=3.0$  m) for the flexible culvert (e.g.,  $F=9.4$ ). A similar trend is observed for the relationship between the  $W_F$  and  $\theta/\gamma_{ff}$ , but with a larger reduction effect. The above results indicate that a further increase in the foundation width of a flexible culvert insignificantly enhances the restrain by the surrounding soil. It shows that culvert with “medium flexibility” (e.g.,  $F=1, 2.8$ ) is more influenced by the foundation width.

## 6. Conclusions

A comparative study on the seismic response of three- and four-sided box culverts embedded in dry soil was

presented using two-dimensional numerical simulations. The numerical model accounted for various burial depths and structural thicknesses. Besides, the effect of the foundation width on the culvert response was investigated. The main results of this study highlighted the significant influence of the bottom slab on the seismic behavior of culverts in terms of accelerations, accumulative energies, racking deformations, rocking rotations, and dynamic earth pressures. The conclusions of this paper were the following ones:

1. The presence of a buried culvert generally amplified the spectral accelerations in the high frequency range due to the kinematic interaction, particularly around the top corner of a flexible three-sided culvert at a shallow depth. As the burial depth and structural stiffness increased, the overall amplification generally reduced.

2. The normalized accumulative energy was amplified around the top corner of the flexible culverts while rigid culverts generally showed a de-amplification effect at a shallow depth. The highest amplification occurred close to the bottom corner of a flexible culvert at deep depths. Compared to four-sided culverts, three-sided culverts demonstrated a relatively large amplification effect.

3. Flexible culverts captured complex racking-rocking responses combined with the inward-outward deformations. Maximum racking ratios and normalized rocking rotations were measured for the more flexible three-sided culvert at a shallow depth. The differences of racking/rocking responses between the three- and four-sided culverts were becoming gradually smaller with increasing burial depth.

4. Three- and four-sided culverts mobilized different earth pressure states of the surrounding soils (active/passive), which were related to the position, burial depth, and flexibility ratio. With the flexibility ratio decreased, the shapes of dynamic earth pressure profiles of four-sided culverts changed from triangular to a three-order polynomial type while the rigid three-sided culverts followed a two-order polynomial shape. The flexible culverts at shallow depths experienced a larger dynamic earth pressure. The maximum difference of the dynamic earth pressures between three- and four-sided culverts was found in the case of flexibility ratio equal to 1, with a value up to ~ 150 %.

5. The racking ratios and normalized rocking rotations of the three-sided culvert are considerably decreased with increasing foundation width, which was more evident for culvert with "medium flexibility". As the foundation width increased, the  $R-F$  and  $\theta/\gamma_{ff}-F$  relations developed for the four-sided culvert could be properly applied as the lower limit for the three-sided culvert.

## Acknowledgments

The authors gratefully acknowledge the financial support provided by the China Scholarship Council (201708130080).

## References

Abuhajar, O., El Naggar, H. and Newson, T. (2015), "Seismic soil-

- culvert interaction", *Can. Geotech. J.*, **52**(11), 1649-1667. <https://doi.org/10.1139/cgj-2014-0494>.
- Acharya, R., Han, J. and Parsons, R.L. (2016b), "Numerical analysis of low-fill box culvert under rigid pavement subjected to static traffic loading", *Int. J. Geomech.*, **16**, 1-14. [https://doi.org/10.1061/\(ASCE\)GM.1943-5622.0000652](https://doi.org/10.1061/(ASCE)GM.1943-5622.0000652).
- Acharya, R., Han, J., Brennan, J.J., Parsons, R.L. and Khatri, D. K. (2016a), "Structural response of a low-fill box culvert under static and traffic loading", *J. Perform. Construct. Facil.*, **30**, 1-7. [https://doi.org/10.1061/\(ASCE\)CF.1943-5509.0000690](https://doi.org/10.1061/(ASCE)CF.1943-5509.0000690).
- An, X., Shawky, A. and Maekawa, K. (1997), "The collapse mechanism of a subway station during the Great Hanshin earthquake", *Cement Concrete Compos.*, **19**, 241-257. [https://doi.org/10.1016/S0958-9465\(97\)00014-0](https://doi.org/10.1016/S0958-9465(97)00014-0).
- Anderson, D.G., Martin, G.R., Lam, I. and Wang, J.N. (2008), "NCHRP 611-Seismic analysis and design of retaining walls, buried structures, slopes, and embankments", Washington, D.C., U.S.A.
- Bilotta, E., Lanzano, G., Madabhushi, S.P.G. and Silvestri, F. (2014), "A numerical Round Robin on tunnels under seismic actions", *Acta Geotechnica*, **9**(4), 563-579. <https://doi.org/10.1007/s11440-014-0330-3>.
- Bobet, A. (2010), "Drained and undrained response of deep tunnels subjected to far-field shear loading", *Tunn. Undergr. Sp. Technol.*, **25**(1), 21-31. <https://doi.org/10.1016/j.tust.2009.08.001>.
- Bobet, A., Fernandez, G., Huo, H. and Ramirez, J. (2008), "A practical iterative procedure to estimate seismic-induced deformations of shallow rectangular structures", *Can. Geotech. J.*, **45**, 923-938. <https://doi.org/10.1139/T08-026>.
- Cilingir, U. and Madabhushi, S.P.G. (2011), "Effect of depth on the seismic response of square tunnels", *Soils Found.*, **51**, 449-457. <https://doi.org/10.3208/sandf.51.449>.
- Debiasi, E., Gajo, A. and Zonta, D. (2013), "On the seismic response of shallow-buried rectangular structures", *Tunn. Undergr. Sp. Technol.*, **38**, 99-113. <https://doi.org/10.1016/j.tust.2013.04.011>.
- Deng, Y. H., Dashti, S., Hushmand, A., Davis, C. and Hushmand, B. (2016), "Seismic response of underground reservoir structures in sand: Evaluation of Class-C and C1 numerical simulations using centrifuge experiments", *Soil Dyn. Earthq. Eng.*, **85**, 202-216. <https://doi.org/10.1016/j.soildyn.2016.04.003>.
- Do, N.A., Dias, D., Oreste, P. and Djeran-Maigre, I. (2014a), "2D numerical investigations of twin tunnel interaction", *Geomech. Eng.*, **6**(3), 263-275. <https://doi.org/10.12989/gae.2014.6.3.263>.
- Do, N.A., Dias, D., Oreste, P. and Djeran-Maigre, I. (2015), "Behaviour of segmental tunnel linings under seismic loads studied with the hyperstatic reaction method", *Soil Dyn. Earthq. Eng.*, **79**, 108-117. <https://doi.org/10.1016/j.soildyn.2015.09.007>.
- Do, N. A., Oreste, P., Dias, D., Antonello, C. and Djeran-Maigre, I. (2014b), "Stress and strain state in the segmental linings during mechanized tunnelling", *Geomech. Eng.*, **7**(1), 75-85. <https://doi.org/10.12989/gae.2014.7.1.075>.
- Ertugrul, O.L. (2016), "Numerical modeling of the seismic racking behavior of box culverts in dry cohesionless soils", *KSCE J. Civ. Eng.*, **20**(5), 1737-1746. <https://doi.org/10.1007/s12205-015-0235-1>.
- Golpasand, M.B., Do, N.A., Dias, D. and Nikudel, M.R. (2018), "Effect of the lateral earth pressure coefficient on settlements during mechanized tunneling", *Geomech. Eng.*, **16**(6), 643-654. <https://doi.org/10.12989/gae.2018.16.6.643>.
- Hashash, Y.M.A., Hook, J.J., Schmidt, B. and Yao, J.I.C. (2001), "Seismic design and analysis of underground structures", *Tunn. Undergr. Sp. Technol.*, **16**, 247-293. [https://doi.org/10.1016/S0886-7798\(01\)00051-7](https://doi.org/10.1016/S0886-7798(01)00051-7).

- Huo, H., Bobet, A., Fernández, G. and Ramírez, J. (2005), "Load transfer mechanisms between underground structure and surrounding ground: Evaluation of the failure of the Daikai station", *J. Geotech. Geoenviron. Eng.*, **131**(12), 1522-1533. [https://doi.org/10.1061/\(ASCE\)1090-0241\(2005\)131:12\(1522\)](https://doi.org/10.1061/(ASCE)1090-0241(2005)131:12(1522)).
- Huo, H., Bobet, A., Fernández, G. and Ramírez, J. (2006), "Analytical solution for deep rectangular structures subjected to far-field shear stresses", *Tunn. Undergr. Sp. Technol.*, **21**(6), 613-625. <https://doi.org/10.1016/j.tust.2005.12.135>.
- Hushmand, A., Dashti, S., Davis, C., Hushmand, B., McCartney, J. S., Hu, J. and Lee, Y. (2016a), "Seismic performance of underground reservoir structures: insight from centrifuge modeling on the influence of backfill soil type and geometry", *J. Geotech. Geoenviron. Eng.*, **142**(11), 04016058-1. [https://doi.org/10.1061/\(ASCE\)GT.1943-5606.0001544](https://doi.org/10.1061/(ASCE)GT.1943-5606.0001544).
- Hushmand, A., Dashti, S., Davis, C., Hushmand, B., Zhang, M., Ghayoomi, M., McCartney, J.S., Lee, Y. and Hu, J. (2016b), "Seismic performance of underground reservoir structures: Insight from centrifuge modeling on the influence of structure stiffness", *J. Geotech. Geoenviron. Eng.*, **142**(7), 04016020. [https://doi.org/10.1061/\(ASCE\)GT.1943-5606.0001477](https://doi.org/10.1061/(ASCE)GT.1943-5606.0001477).
- Hushmand, A., Dashti, S., Davis, C., McCartney, J.S. and Hushmand, B. (2016c), "A centrifuge study of the influence of site response, relative stiffness, and kinematic constraints on the seismic performance of buried reservoir structures", *Soil Dyn. Earthq. Eng.*, **88**, 427-438. <https://doi.org/10.1016/j.soildyn.2016.06.011>.
- Iidai, H., Hirotoi, T. and Iwafuji, M. (1996), "Damage to Daikai subway station", *Soils Found.*, **36**, 283-300. <https://doi.org/10.3208/sandf.36.Special.283>.
- Itasca. (2011), *Software Manual of FLAC Version 7.0*, Itasca Consulting Group.
- Kim, K. and Yoo, C.H. (2005), "Design loading on deeply buried box culverts", *J. Geotech. Geoenviron. Eng.*, **131**(1), 20-27. [https://doi.org/10.1061/\(ASCE\)1090-0241\(2005\)131:1\(20\)](https://doi.org/10.1061/(ASCE)1090-0241(2005)131:1(20)).
- Kuhlemeyer, R.L. and Lysmer, J. (1973), "Finite element method accuracy for wave propagation problems", *J. Soil Mech. Found. Div.*, **99**, 421-427.
- Kwok, A.O.L., Stewart, J.P., Hashash, Y.M.A., Matasovic, N., Pyke, R., Wang, Z.L. and Yang, Z.H. (2007), "Use of exact solutions of wave propagation problems to guide implementation of nonlinear seismic ground response analysis procedures", *J. Geotech. Geoenviron. Eng.*, **133**(11), 1385-1398. [https://doi.org/10.1061/\(ASCE\)1090-0241\(2007\)133:11\(1385\)](https://doi.org/10.1061/(ASCE)1090-0241(2007)133:11(1385)).
- Lancioni, G., Bernrtti, R., Quagliarini, E. and Tonti, L. (2014), "Effects of underground cavities on the frequency spectrum of seismic shear waves", *Adv. Civ. Eng.*, 934284. <https://doi.org/10.1155/2014/934284>.
- Li, T.Z. and Yang, X.L. (2019), "Face stability analysis of rock tunnels under water table using Hoek-Brown failure criterion", *Geomech. Eng.*, **18**(3), 235-245. <https://doi.org/10.12989/gae.2019.18.3.235>.
- Liu, N.N., Huang, Q.B., Fan, W., Ma, Y.J. and Peng, J.B. (2018), "Seismic responses of a metro tunnel in a ground fissure site", *Geomech. Eng.*, **15**(2), 775-781. <https://doi.org/10.12989/gae.2018.15.2.775>.
- Moss, R.E.S. and Crosariol, V.A. (2013), "Scale model shake table testing of an underground tunnel cross section in soft clay", *Earthq. Spectr.*, **29**(4), 1413-1440. <https://doi.org/10.1193/070611EQS162M>.
- Owen, G.N. and Scholl, R.E. (1981), *FHWA/RD-80/195-Earthquake Engineering of Large Underground Structures*.
- Parra-Montesinos, G.J., Bobet, A. and Ramirez, J.A. (2006), "Evaluation of soil-structure interaction and structural collapse in Daikai subway station during Kobe earthquake", *ACI Struct. J.*, **103**(1), 113-122.
- Penzien, J. (2000), "Seismically induced racking of tunnel linings", *Earthq. Eng. Struct. Dyn.*, **29**(5), 683-691. [https://doi.org/10.1002/\(SICI\)1096-9845\(200005\)29:5<683::AID-EQE932>3.0.CO;2-1](https://doi.org/10.1002/(SICI)1096-9845(200005)29:5<683::AID-EQE932>3.0.CO;2-1).
- Penzien, J. and Wu, C.L. (1998), "Stresses in linings of bored tunnels", *Earthq. Eng. Struct. Dyn.*, **27**(3), 283-300. [https://doi.org/10.1002/\(SICI\)1096-9845\(199803\)27:3<283::AID-EQE732>3.0.CO;2-T](https://doi.org/10.1002/(SICI)1096-9845(199803)27:3<283::AID-EQE732>3.0.CO;2-T).
- Sadek, M. and Shahrou, I. (2006), "Influence of the head and tip connection on the seismic performance of micropiles", *Soil Dyn. Earthq. Eng.*, **26**(5), 461-468. <https://doi.org/10.1016/j.soildyn.2005.10.003>.
- Seylabi, E. E., Jeong, C., Dashti, S., Hushmand, A. and Taciroglu, E. (2018), "Seismic response of buried reservoir structures: A comparison of numerical simulations with centrifuge experiments", *Soil Dyn. Earthq. Eng.*, **109**, 89-101. <https://doi.org/10.1016/j.soildyn.2018.03.003>.
- Shahrou, I., Khoshnoudian, F., Sadek, M. and Mroueh, H. (2010), "Elastoplastic analysis of the seismic response of tunnels in soft soils", *Tunn. Undergr. Sp. Technol.*, **25**(4), 478-482. <https://doi.org/10.1016/j.tust.2010.01.006>.
- Sharma, S. and Judd, W.R. (1991), "Underground opening damage from earthquakes", *Eng. Geol.*, **30**, 263-276. [https://doi.org/10.1016/0013-7952\(91\)90063-Q](https://doi.org/10.1016/0013-7952(91)90063-Q).
- Sun, Q. Q. and Dias, D. (2019b), "Seismic behavior of circular tunnels: Influence of the initial stress state", *Soil Dyn. Earthq. Eng.*, **126**, 105808. <https://doi.org/10.1016/j.soildyn.2019.105808>.
- Sun, Q.Q., Dias, D. and e Sousa, L.R. (2020), "Soft soil layer-tunnel interaction under seismic loading", *Tunn. Undergr. Sp. Technol.*, **98**, 103329. <https://doi.org/10.1016/j.tust.2020.103329>.
- Sun, Q.Q., Dias, D., Guo, X. and Li, P. (2019b), "Numerical study on the effect of a subway station on the surface ground motion", *Comput. Geotech.*, **111**, 243-254. <https://doi.org/10.1016/j.compgeo.2019.03.026>.
- Sun, Q.Q. and Dias, D. (2018), "Significance of Rayleigh damping in nonlinear numerical seismic analysis of tunnels", *Soil Dyn. Earthq. Eng.*, **115**, 489-494. <https://doi.org/10.1016/j.soildyn.2018.09.013>.
- Sun, Q.Q. and Dias, D. (2019a), "Assessment of stress relief during excavation on the seismic tunnel response by the pseudo-static method", *Soil Dyn. Earthq. Eng.*, **117**, 384-397. <https://doi.org/10.1016/j.soildyn.2018.09.019>.
- Sun, Q.Q., Bo, J.S. and Dias, D. (2019a), "Viscous damping effects on the seismic elastic response of tunnels in three sites", *Geomech. Eng.*, **18**(6), 639-650. <https://doi.org/10.12989/gae.2019.18.6.639>.
- Sun, Q.Q., Bo, J.S., Sun, Y.W. and Zhang, Z.P. (2016), "A state-of-the-art review of seismic response analysis of tunnels", *World Earthq. Eng.*, **32**, 159-169 (in Chinese). [https://doi.org/1007-6069\(2016\)02-0159-11](https://doi.org/1007-6069(2016)02-0159-11).
- Sun, Q.Q., Dias, D. and e Sousa, L.R. (2019c), "Impact of an underlying soft soil layer on tunnel lining in seismic conditions", *Tunn. Undergr. Sp. Technol.*, **90**, 293-308. <https://doi.org/10.1016/j.tust.2019.05.011>.
- Tsinidis, G. (2017), "Response characteristics of rectangular tunnels in soft soil subjected to transversal ground shaking", *Tunn. Undergr. Sp. Technol.*, **62**, 1-22. <https://doi.org/10.1016/j.tust.2016.11.003>.
- Tsinidis, G. and Ptilakis, K. (2018), "Improved R-F relations for the transversal seismic analysis of rectangular tunnels", *Soil Dyn. Earthq. Eng.*, **107**, 48-65. <https://doi.org/10.1016/j.soildyn.2018.01.004>.
- Tsinidis, G., Ptilakis, K. and Madabhushi, S.P.G. (2016a), "On the dynamic response of square tunnels in sand", *Eng. Struct.*, **125**, 419-437. <https://doi.org/10.1016/j.engstruct.2016.07.014>.

- Tsinidis, G., Rovithis, E., Pitilakis, K. and Chazelas, J. (2015), "Dynamic response of square tunnels: Centrifuge testing and validation of existing design methodologies", *Geotechnique*, **65**, 401-417. <https://doi.org/10.1680/geot.SIP.15.P.004>.
- Tsinidis, G., Rovithis, E., Pitilakis, K. and Chazelas, J.L. (2016b), "Seismic response of box-type tunnels in soft soil: Experimental and numerical investigation", *Tunn. Undergr. Sp. Technol.*, **59**, 199-214. <https://doi.org/10.1016/j.tust.2016.07.008>.
- Ulgen, D., Saglam, S. and Ozkan, M.Y. (2015a), "Assessment of racking deformation of rectangular underground structures by centrifuge tests", *Geotechnique Lett.*, **5**(4), 261-268. <https://doi.org/10.1680/jgele.15.00097>.
- Ulgen, D., Saglam, S. and Ozkan, M.Y. (2015b), "Dynamic response of a flexible rectangular underground structure in sand: Centrifuge modeling", *Bull. Earthq. Eng.*, **13**(9), 2547-2566. <https://doi.org/10.1007/s10518-015-9736-z>.
- Wang, C.J. (2011), "Seismic racking of a dual-wall subway station box embedded in soft soil strata", *Tunn. Undergr. Sp. Technol.*, **26**(1), 83-91. <https://doi.org/10.1016/j.tust.2010.05.003>.
- Wang, J.N. (1993), *Seismic Design of Tunnels: A Simple State-of-the-Art Design Approach*, Parsons, Brinckerhoff, Quade and Douglas Inc., New York, U.S.A.
- Wang, W.L., Wang, T.T., Su, J.J., Lin, C.H., Seng, C.R. and Huang, T.H. (2001), "Assessment of damage in mountain tunnels due to the Taiwan Chi-Chi Earthquake", *Tunn. Undergr. Sp. Technol.*, **16**(3), 133-150. [https://doi.org/10.1016/S0886-7798\(01\)00047-5](https://doi.org/10.1016/S0886-7798(01)00047-5).
- Yang, X.L. and Huang, F. (2011), "Collapse mechanism of shallow tunnel based on nonlinear Hoek-Brown failure criterion", *Tunn. Undergr. Sp. Technol.*, **26**(6), 686-691. <https://doi.org/10.1016/j.tust.2011.05.008>.
- Yang, X.L. and Wang, J.M. (2011), "Ground movement prediction for tunnels using simplified procedure", *Tunn. Undergr. Sp. Technol.*, **26**(3), 462-471. <https://doi.org/10.1016/j.tust.2011.01.002>.
- Yang, X.L. and Yin, J.H. (2005), "Upper bound solution for ultimate bearing capacity with a modified Hoek-Brown failure criterion", *Int. J. Rock Mech. Min. Sci.*, **42**(4), 550-560. <https://doi.org/10.1016/j.ijrmms.2005.03.002>.
- Yang, X.L. and Yin, J.H. (2010), "Slope equivalent Mohr-Coulomb strength parameters for rock masses satisfying the Hoek-Brown criterion", *Rock Mech. Rock Eng.*, **39**, 505-511. <https://doi.org/10.1007/s00603-009-0044-2>.
- Youd, T.L. and Beckman, C.J. (1996), "Highway culvert performance during past earthquake", NCEER-96-0015, Buffalo, New York, U.S.A.
- Yu, H.T., Chen, J.T., Bobet, A. and Yuan, Y. (2016), "Damage observation and assessment of the Longxi tunnel during the Wenchuan earthquake", *Tunn. Undergr. Sp. Technol.*, **54**, 102-116. <https://doi.org/10.1016/j.tust.2016.02.008>.
- Zhang, B., Ma, Z.Y., Wang, X., Zhang, J.S. and Peng, W.P. (2020), "Reliability analysis of anti-seismic stability of 3D pressurized tunnel faces by response surfaces method", *Geomech. Eng.*, **20**(1), 43-54. <https://doi.org/10.12989/gae.2020.20.1.043>.
- Zhang, B., Wang, X., Zhang, J.S. and Meng, F. (2017), "Three-dimensional limit analysis of seismic stability of tunnel face with quasi-static method", *Geomech. Eng.*, **13**(2), 301-318. <https://doi.org/10.12989/gae.2017.13.2.301>.